

Effect of draw solution type and operational mode of forward osmosis with laboratory-scale membranes and a spiral wound membrane module

E. R. Cornelissen, D. J. H. Harmsen, E. F. Beerendonk, J. J. Qin and J. W. M. N. Kappelhof

ABSTRACT

Forward osmosis (FO) is a concentration driven membrane process which recently gained an increase in attention due to the development of improved FO membranes. Most of the currently available data on FO research is obtained on small laboratory-scale set-ups, thereby overlooking the effects of scaling-up to pilot or full-scale size. In this paper, FO experiments are carried out with a 10.16 cm (4-in) spiral wound FO (SWFO) Hydration Technologies Innovations (HTI) module. The performance of the SWFO module was investigated during daily experiments and the influence of two types of draw solutions (NaCl and MgCl₂) was evaluated and compared to data from lab-scale FO research. Furthermore, the difference between fixed draw solution concentration and draw solution dilution was studied for both draw solutions. Salt flux was determined from the increase in: (i) conductivity; and (ii) individual ion concentration in the feed vessel. Water and salt flux values from laboratory-scale membrane FO experiments were similar but slightly lower than that of the SWFO module in the fixed draw solution concentration experiments (respectively 5 L/m²h and 3 g/m²h for 0.5 M NaCl). Salt flux values obtained from individual ion measurements were lower and more accurate compared to that determined by conductivity measurements.

Key words | forward osmosis, osmotic driving force, salt flux, spiral wound membrane elements, water flux

ABBREVIATIONS

DI de-mineralised water
FO forward osmosis
ICP internal concentration polarization
SWFO spiral wound forward osmosis

T temperature (°C)
 V_f feed volume (L)
 V_p permeate volume (L)
 V_s concentrated salt solution volume (L)
 Δt elapsed time (h)

LIST OF SYMBOLS

A_m membrane area (m²)
 c concentration (M)
 J_s salt flux (g/m²h)
 J_w water flux (L/m²h)
 n number of experiments (-)

doi: 10.2166/wrd.2011.042

E. R. Cornelissen (corresponding author)
D. J. H. Harmsen
E. F. Beerendonk
KWR Watercycle Research Institute,
P.O. Box 1072,
3430 BB Nieuwegein,
The Netherlands
E-mail: emile.cornelissen@kwrwater.nl

J. J. Qin
Technology & Water Quality Office,
Public Utilities Board,
82 Toh Guan Road East #C4-03,
Singapore 608575

J. W. M. N. Kappelhof
Waternet,
Korte Ouderkerkerdijk 7,
1096 AC Amsterdam,
The Netherlands

INTRODUCTION

Forward osmosis (FO) is an emerging membrane process which is proposed for different technologies, such as desalination (McGinnis & Elimelech 2007), wastewater treatment (Cornelissen *et al.* 2008; Achilli *et al.* 2009), reuse of

wastewater (Cath *et al.* 2005) and the concentration of fruit juices (Babu *et al.* 2006). Advantages of FO are: (i) low energy consumption; (ii) high product quality; and (iii) lower fouling propensity compared with state of the art pressure driven membrane processes. An increasing amount of research is devoted to the application of FO for different and new technologies and to the fundamental understanding of underlying separation and fouling mechanisms (Mi & Elimelech 2008; Lay *et al.* 2010; Tang *et al.* 2010). Most of the (published) research is, however, conducted on a relatively small laboratory scale using FO membranes with a membrane area of typically smaller than 0.1 m². Problems encountered when scaling up the results to pilot or full-scale applications are usually neglected. The first, and to the best of the authors' knowledge only, published paper on a spiral wound FO (SWFO) membrane element to date emphasises on water flux measurements and modelling (Xu *et al.* 2010). It is important to note that in this work dilution of the bulk draw solution concentration by the permeate flow in the SWFO module was recognised, resulting in a reduced flux performance compared to small laboratory scale FO experiments.

In this paper experiments were described with one of the first commercially available SWFO membrane modules (HTI). The pilot-scale experiments were carried out in a period from May till September 2009 with locally available tap water at the KWR facility in Nieuwegein (The Netherlands). The performance of the SWFO module was investigated during daily experiments, and the influence of two types of draw solutions (NaCl and MgCl₂) was evaluated and compared with data from laboratory scale FO research. Furthermore, the difference between fixed draw solution concentrations and draw solution dilution was studied for both draw solutions. Salt flux was determined from the increase in: (i) conductivity; and (ii) individual ion concentration in the feed vessel.

EXPERIMENTAL METHODS

Laboratory and pilot set-up

FO laboratory experiments were carried out in a U-tube set-up and are described elsewhere in more detail

(Cornelissen *et al.* 2008) (Figure 1). FO pilot-scale experiments were carried out in an adapted pilot scale set-up for FO research (Cornelissen *et al.* 2010a). Locally available drinking water was pretreated with a 1- μ m filter (1 micron melt blown filter, type A7PP001-09NN from Van Borselen). Drinking water was directly fed with a feed pump (Calpeda), to the entrance of the membrane module: (i) in a single pass mode; or (ii) to a stainless steel vessel for recirculation over the membrane module. The temperature of the feed solution was controlled at 20 °C (using a Tamson TLC 40 cooler) during recirculation experiments. Recirculation was necessary to determine the salt flux at the feed side of the membrane module. The pressure of the feed was directly measured by pressure indicators (Cerapahrit T from E + H) before entering the SWFO membrane module.

The draw solution was re-circulated over the membrane using an air pump (Verder Air VA15-Verder). The concentration of the draw solution was kept constant during pilot-scale testing by dosage of a concentrated salt solution into an open vessel in the draw solution loop using a dosing pump (Masterflex L/S). The volume decrease of the concentrated salt solution vessel was recorded by a mass balance (Satex, SA 250). Conductivity was measured with conductivity meters (Liquisys M CLM223/253 transmitter with Indumax P CLS50 sensors – E + H) positioned: (i) before the SWFO membrane module at the feed side; and (ii) before and after the membrane module at the draw side. The volume increase in the draw solution loop as a result of FO permeation was registered by an electromagnetic flow



Figure 1 | The pilot-scale FO set-up and the SWFO membrane module at the KWR pilot facility in Nieuwegein.

measuring system (Proline Promag 50 – E + H) registering the overflow of an open vessel within the draw solution loop. An air compressor was provided at the feed entrance of the SWFO membrane module to facilitate aeration of the feed channel of the SWFO membrane module.

A data-logger (Memograph M – E + H) was installed in the control panel of the pilot-scale set-up to continuously monitor and record: (i) the permeate flow from the overflow vessel; (ii) feed water conductivity and temperature; (iii) draw solution conductivity; and (iv) temperature before and after dosing concentrated draw solution into the draw solution loop.

Membranes

A 10.16 cm (4") SWFO membrane module (HTI) constructed of cellulose triacetate embedded in a polyester screen mesh (www.htiwater.com) was used. According to the manufacturer, the SWFO module consists of a Naltex-type feed spacer with a thickness of 1.17 mm (0.046"), 3 × 3 cm strands per cm (7.5 × 7.5 strands per inch) (diamond squared) and 0.76 mm (0.030")-diameter polypropylene fibers. The SWFO module has an effective membrane area of 3.3 m². Recommended flow rates are 18 L/min feed flow (at 70–110 kPa) and 6 L/min draw flow (at 50 kPa). Pressure drops are proportional to flow rates, and the feed side should be at a higher pressure than the draw side. The minimum draw feed rate is not established yet, but it is probably around 1 L/min.

Chemicals

De-mineralised water (DI water) was available at the KWR facility in Nieuwegein, obtained from a de-mineralisation installation using softening followed by reverse osmosis and cation and anion exchange. DI water has a conductivity of less than 0.15 µS/cm. Drinking water was available at the KWR facility in Nieuwegein (for specifications see [Cornelissen *et al.* 2010b](#)). Sodium chloride (NaCl): (Akzo Nobel, Industrial salt compacted 25 kg), magnesium chloride (MgCl₂·6H₂O): (Merck, 25 kg) and sodium metabisulfite (Na₂S₂O₅) (J. T. Baker) were used for the draw or preservation solutions.

Experimental test conditions

Feed water and draw solution flow during the pilot-scale experiments was 1,000 and 300–360 L/h, respectively. The feed pressure before the membrane element was measured at the beginning and the end of an experiment. To verify the concentration of the draw solution during the pilot experiment, the concentration was determined at the beginning and at the end of each experiment by temperature corrected (20 °C) conductivity measurement (Radiometer CDM 83) using a calibration curve for each type of (single) salt solution. The pH (Orion 720A pH meter) of the draw solution was measured at the beginning and the end of the experiments. Experiments were conducted at local temperature with a maximum duration of 7 h. At the end of a run the membrane module was filled with drinking water to prevent drying of the membrane. For storage of more than one day the membrane module was filled with 10 g/L sodium metabisulfite.

Data processing

The volumetric water flux was determined by a mass balance in the draw solution loop and given by:

$$J_w = \frac{V_p - V_s}{A_m \Delta t} \quad (1)$$

where J_w is the water flux (L/m²h), V_p is the permeate volume (L), V_s is the concentrated salt solution volume (L), A_m is the membrane area (m²) and Δt is the elapsed time.

The salt flux (J_s in g/m²h) was determined from the increase of the conductivity in the feed water compartment. The salt flux was directed in the opposite direction from the water flux, from the draw solution side to the feed water side. The salt flux was given by:

$$J_s = \frac{\Delta(c_f V_f)}{A_m \Delta t} \quad (2)$$

where J_s is the salt flux (L/m²h), c_f is the feed concentration and V_f is the feed volume (L).

A series of experiments was conducted during the period of August to September 2009 to study the influence

of draw solution dilution on the water and salt flux. Due to practical restrictions, experiments were only conducted during the daytime and started up again the next day. Every experiment took 3 days due to a limited permeate flow.

To validate the conductivity measurements, additional feed analyses were taken. Different ions (Na^+ and Cl^- for the NaCl experiment and Mg^{2+} and Cl^- for the MgCl_2 experiment) were analysed. Na^+ and Mg^{2+} were analysed at the KWR laboratory in Nieuwegein using the inductively coupled plasma mass spectrometry (ICP-MS) (KWR method; LAM058, using a Perkin Elmer ICP-MS type ELAN6000). Cl^- was analysed at the Vitens laboratory in Leeuwarden using a discrete photometric analyzer (analysed according to NEN6604:2007, Thermo Scientific Aquakem 600 Photometric Analyser). From these analyses, the individual ion fluxes were calculated and compared to the indicative salt flux determined from conductivity measurements.

RESULTS AND DISCUSSION

Performance of the spiral wound FO membrane

Daily FO recirculation experiments were conducted with drinking water using the SWFO membrane module. The permeate flow rate kept constant during these runs at approximately 17–18 L/h (Figure 2), which resulted in a water flux of 4.7 L/m²h. The conductivity in the feed vessel increased 150 $\mu\text{S}/\text{cm}$ during the experiment of 5.5 h

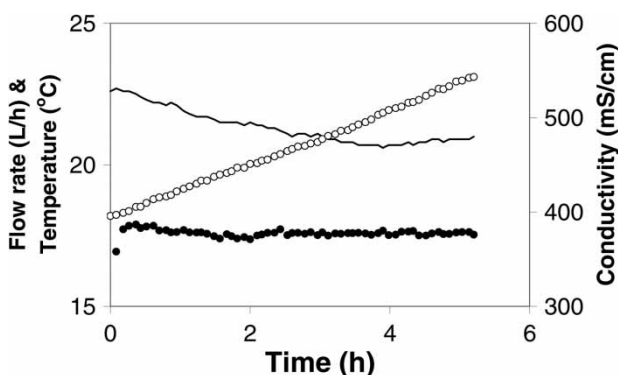


Figure 2 | Permeate flow rate (black), feed vessel conductivity (white) and temperature (line) in function of time (feed: drinking water; draw solution: 0.5 M NaCl; temperature: 20 ± 2 °C).

(Figure 2), from which a salt flux of 3.0 g/m²h can be calculated using the NaCl calibration curve. Temperature values varied slightly between 20 and 23 °C, and were used for temperature correction of the water and salt flux data (Cornelissen *et al.* 2010b).

For 0.5 M MgCl_2 , similar experiments were carried out, resulting in water and salt flux values of 5.4 L/m²h and 2.0 g/m²h (results not shown here).

Influence of draw solution type for lab-scale membranes and SWFO module

The average performance of the laboratory scale membranes and SWFO membrane module depends on the draw solution type (Figures 3 and 4). Under similar experimental conditions the water flux is similar for 0.5 M NaCl and for 0.5 M MgCl_2 , while the salt flux is higher for 0.5 M NaCl. Higher water flux values were expected for 0.5 M MgCl_2 because of: (i) a higher osmotic pressure difference over the membrane; and (ii) a lower internal concentration polarization (ICP) within the FO membrane structure. Similar water flux values were observed for NaCl and MgCl_2 due to large variations in experimental results for the 0.5 M MgCl_2 laboratory experiment. A lower salt flux was due to higher steric hindrance and electrostatic repulsion of MgCl_2 by the FO membrane. While water flux values were similar for laboratory-scale membranes and the SWFO module, the salt flux values were higher for the SWFO module for both draw solutions. This was hypothesised by

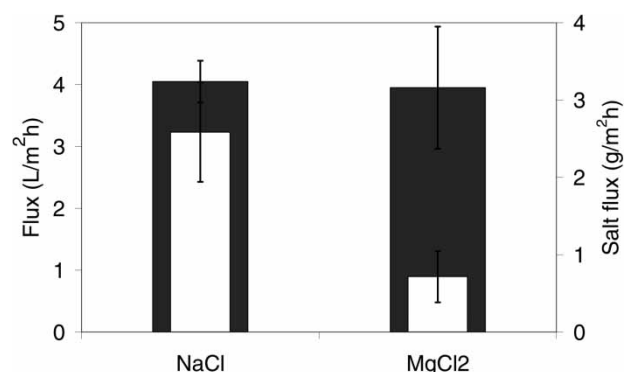


Figure 3 | Water (black) and salt (white) flux for laboratory-scale membranes for two draw solutions (feed: drinking water; draw solution: 0.5 M NaCl and 0.5 M MgCl_2 temperature: 20 ± 2 °C; membrane orientation: active layer facing the feed solution) ($n_{\text{NaCl}} = 12$ and $n_{\text{MgCl}_2} = 4$).

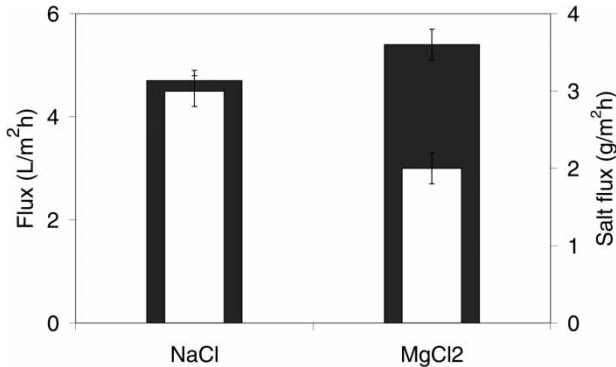


Figure 4 | Water (black) and salt (white) flux for the SWFO membrane module for two draw solutions (feed: drinking water; draw solution: 0.5 M NaCl and 0.5 M MgCl₂; temperature: 20 ± 2 °C; membrane orientation: active layer facing the feed solution) ($n_{\text{NaCl}} = 7$ and $n_{\text{MgCl}_2} = 3$).

external concentration polarization phenomena which were more pronounced for the SWFO module.

Standard deviations are indicated as error bars (Figures 3 and 4), and are relatively small (5%) for the standard deviations of the SWFO module compared with the standard deviations observed during laboratory-scale experiments, due to the relative large membrane area under investigation. One spiral wound FO membrane module was available for these studies.

Draw solution dilution experiments SWFO module

Draw solution dilution experiments were carried out to investigate the influence of a continuous variation in draw solution concentration on the water and salt flux. During these experiments replenishment of the salt load in the draw solution loop is omitted, resulting in a dilution of the draw solution loop in time. Starting concentrations of the draw solutions are 1.1 M NaCl and 0.9 M MgCl₂ and were allowed to dilute in time over a period of 3 (working) days. During night-times the experiment was stopped by replacing the draw solution with drinking water. Prior to the re-start of the experiment the draw solution was replenished by the addition of fresh salt solution (either 1.1 M NaCl or 0.9 M MgCl₂) resulting in a slightly higher draw solution concentration at the start of each working day. As a result of this higher draw solution concentration the water and salt flux values increased. During the actual experiment both water and salt fluxes decreased as a result of decreasing

draw solution concentration for both NaCl (Figure 5) and MgCl₂ (Figure 6).

Water flux values decreased from 8.2 to 3.3 L/m²h for NaCl, while salt flux values decreased from 5.6 to 2.4 g/m²h. The decrease on water flux and salt flux had a similar shape, since both they were both affected by ICP. The J_s/J_w ratio was nearly constant during the experiment, as was observed before by other researchers (Tang *et al.* 2010). Two experiments were carried out which showed a similar behaviour in flux decline as a result of draw solution dilution. The water and salt flux curves were fitted using an empirical relation for NaCl to obtain:

$$J_w = 2.6 \ln(c_{\text{NaCl}}) + 7.8$$

$$J_s = 1.9 \ln(c_{\text{NaCl}}) + 5.3$$

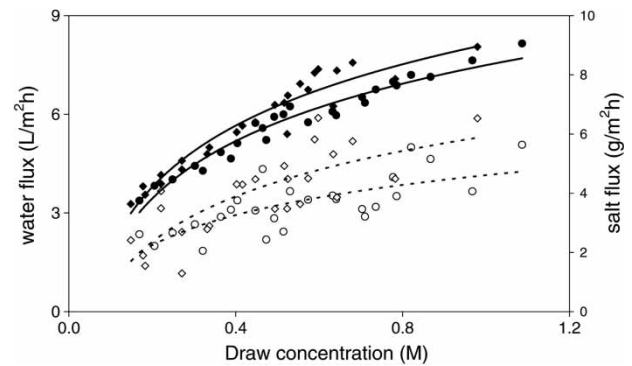


Figure 5 | Water (black) and salt (white) flux values for the SWFO membrane module in function of draw solution concentration (draw solution: NaCl; membrane orientation: active layer facing feed side; temperature: 20 ± 2 °C). Duplicate experiments.

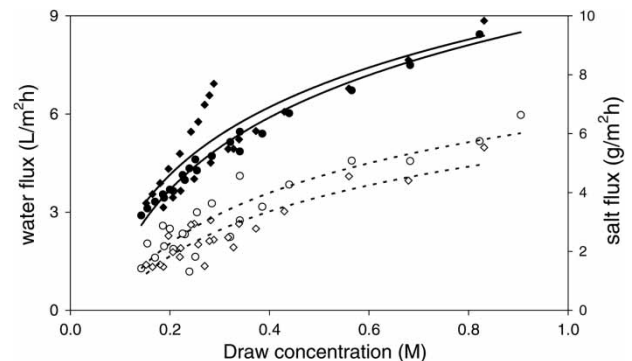


Figure 6 | Water (black) and salt (white) flux values for the SWFO membrane module in function of draw solution concentration (draw solution: MgCl₂; membrane orientation: active layer facing feed side; temperature: 20 ± 2 °C). Duplicate experiments.

The accuracy of the curve fit was high (93–95%) for the water flux of the NaCl experiment, and moderate (54–62%) for the salt flux values. The empirical relation encompasses external and ICP effects which play a role during the FO process. Mass transport models are currently under development to describe the observed phenomena in the SWFO module, which can separate these two phenomena.

Water flux values decreased from 8.9 to 3.3 L/m²h for MgCl₂, while salt flux values decreased from 5.5 to 1.5 g/m²h. Two experiments were carried out which showed a similar behaviour in flux decline as a result of draw solution dilution. Again, a constant J_s/J_w ratio was observed (Zou *et al.* 2011). The water and salt flux curves were fitted using an empirical relation for MgCl₂ to obtain:

$$J_w = 3.1 \ln(c_{\text{MgCl}_2}) + 8.9$$

$$J_s = 2.2 \ln(c_{\text{MgCl}_2}) + 5.5$$

The accuracy of the curve fit was high (74–98%) for the water flux of the MgCl₂ experiment, and moderate (82–83%) for the salt flux values. The reason for the inaccuracy was ascribed to the increase in water and salt flux overnight due to the addition of fresh salt solution to the draw solution at the re-start of the experiment at the start of a working day, as described above.

The water and salt flux values determined at constant draw solution concentration (Figures 3 and 4) were compared with water and salt flux values determined with draw solution dilution (Figures 5 and 6 and Table 1). Water flux and salt flux values are significantly higher for the draw solution dilution experiments. An explanation for this observation could not be found.

During the draw solution dilution experiments, feed water samples were taken in time which were analysed on

NaCl and MgCl₂ concentration for the two different experiments. Salt flux values were calculated on the basis of the increase in NaCl (Figure 7) and MgCl₂ (Figure 8) concentrations in the feed water vessel in time. A similar decrease in salt flux was observed in the function of the draw solution dilution, as for salt flux values determined from conductivity measurements in the feed vessel. The salt flux values determined by feed water analysis, however, were significantly lower than that determined by conductivity measurements, probably as a result of interfering ions when measuring the conductivity (Hancock & Cath 2009).

Salt flux values decreased from 4.8 to 1.4 g/m²h for NaCl, and decreased from 1.2 to 0.3 g/m²h for MgCl₂. The salt flux curves were fitted for NaCl and MgCl₂ to obtain:

$$J_s = 1.6 \ln(c_{\text{NaCl}^-}) + 4.3$$

$$J_s = 0.4 \ln(c_{\text{MgCl}_2}) + 1.2$$

The accuracy of the curve fit was high (83 and 93%) for both the NaCl and MgCl₂ experiments. Salt flux determination on the basis of individual ion analysis proved to be more accurate than salt flux determination based upon conductivity measurements.

The salt flux values determined at constant draw solution concentration (Figure 4) were compared with salt flux values determined with draw solution dilution by individual ion concentration measurement (Table 1). Salt flux values are similar for the draw solution dilution experiments. A better performance was found when 0.5 M MgCl₂ draw solutions were used compared with 0.5 M NaCl draw solutions (higher water flux combined with a lower salt water flux).

Table 1 | Water and salt flux values from (i) constant draw solution experiment and (ii) dilution draw solution experiment

Experiment type	Operational mode	NaCl (0.5 M)		MgCl ₂ (0.5 M)	
		J_w (L/m ² h)	J_s (g/m ² h)	J_w (L/m ² h)	J_s (g/m ² h)
Lab-scale membrane	Constant draw concentration	4.0	2.6	3.9	1.0
SWFO module	Constant draw concentration	4.7	3.0	5.4	2.0
SWFO module	Dilutive draw concentration	6.0	4.0	6.8	4.0
SWFO module	Dilutive draw concentration ^a	–	3.2	–	0.9

^aSalt flux values determined on the basis of individual ion concentrations.

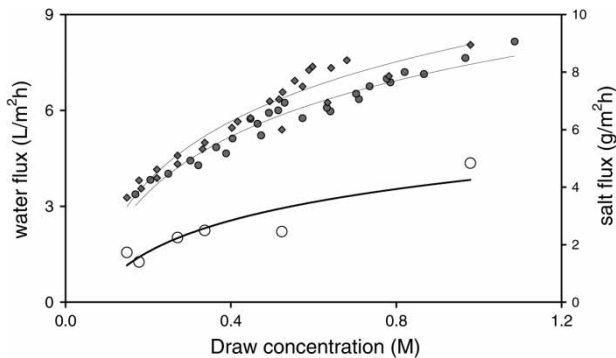


Figure 7 | Salt (white) and water (black) flux values for the SWFO membrane module in function of draw solution concentration as determined from NaCl analysis (draw solution: NaCl; membrane orientation: active layer facing feed side; temperature: 20 ± 2 °C).

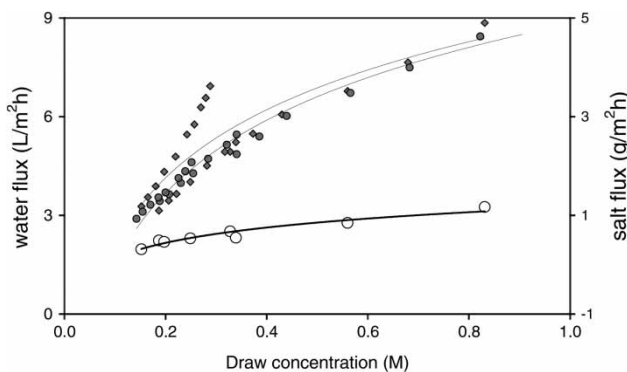


Figure 8 | Salt (white) and water (black) flux values for the SWFO membrane module in function of draw solution concentration as determined from MgCl₂ analysis (draw solution: MgCl₂; membrane orientation: active layer facing feed side; temperature: 20 ± 2 °C).

CONCLUSIONS

One of the first available spiral wound FO membrane modules was acquired and investigated in an on-site pilot research using locally available tap water. The following findings are summarised on the basis of this study.

- Water and salt flux values from laboratory-scale membrane FO experiments were similar to, but slightly lower, for the SWFO module results for the constant draw solution concentration experiments.
- A similar water flux with 0.5 M MgCl₂ was explained by a higher osmotic pressure difference over the membrane, compensated by a lower ICP within the FO membrane structure. A lower salt flux was due to higher steric

hindrance and electrostatic repulsion of MgCl₂ by the FO membrane.

- Water and salt flux values decreased in function of a dilution of the draw solution for both NaCl and MgCl₂. Curve fits were accurate for the water flux curves (>74%) and less accurate for salt flux curves (54–83%) based on conductivity measurements.
- Water flux and salt flux values determined from constant draw solution experiments were significantly lower compared with water flux and salt flux values determined by draw solution dilution experiments.
- Additional salt flux values were obtained during draw solution dilution experiments by individual ion measurements in the feed vessel during the experiment, which provided lower and more accurate salt flux values compared to salt flux values determined by conductivity measurements.

ACKNOWLEDGEMENTS

The authors acknowledge the support of SenterNovem of the Dutch Ministry of Economic Affairs (project number ISO54040). The authors also acknowledge the support of the Innovation for Environmental Sustainability Fund of the National Environment Agency, Singapore (project number NEA/EP/PDD/05-13097). The authors thank Keith Lampi (HTI) and Ed Beaudry (HTI) for additional information on the SWFO module. Finally, Hugo Veysière (INSA Toulouse) is acknowledged for carrying out the experimental work to fulfill the requirements for his thesis.

REFERENCES

- Achilli, A., Cath, T. Y., Marchand, E. A. & Childress, A. E. 2009 *The forward osmosis membrane bioreactor: a low fouling alternative to MBR processes*. *Desalination* **238** (1–3), 10–21.
- Babu, B. R., Rastogi, N. K. & Raghavarao, K. S. 2006 *Effect of process parameters on transmembrane flux during direct osmosis*. *J. Memb. Sci.* **280** (1–2), 185–194.
- Cath, T. Y., Gormly, S., Beaudry, E. G., Flynn, M. T., Adams, V. D. & Childress, A. E. 2005 *Membrane contactor processes for wastewater reclamation in space: part I. Direct osmotic concentration as pretreatment for reverse osmosis*. *J. Memb. Sci.* **257** (1–2), 85–98.

- Cornelissen, E. R., Chasseriaud, D., Siegers, W. G., Beerendonk, E. F. & van der Kooij, D. 2010a [Effect of anionic fluidized ion exchange \(FIX\) pre-treatment on nanofiltration \(NF\) membrane fouling](#). *Water Res.* **44** (10), 3283–3293.
- Cornelissen, E. R., Harmsen, D., Beerendonk, E. F., Qin, J. J., Oo, H., de Korte, K. F. & Kappelhof, J. W. N. M. 2010b [The innovative Osmotic Membrane Bioreactor \(OMBR\) for reuse of wastewater](#). *Water Sci. Technol.: Water Supply* **63** (8), 1557–1565.
- Cornelissen, E. R., Harmsen, D., de Korte, K. F., Ruiken, C. J., Qin, J. J., Oo, H. & Wessels, L. P. 2008 [Membrane fouling and process performance of forward osmosis membranes on activated sludge](#). *J. Memb. Sci.* **319** (1–2), 158–168.
- Hancock, N. T. & Cath, T. Y. 2009 [Solute coupled diffusion in osmotically driven membrane processes](#). *Environ. Eng. Sci.* **43**, 6769–6775.
- Lay, W. C. L., Chong, T. H., Tang, C. Y., Fane, A. G., Zhang, J. & Liu, Y. 2010 [Fouling propensity of forward osmosis: investigation of the slower flux decline phenomenon](#). *Water Sci. Technol.* **61**, 927–936.
- McGinnis, R. L. & Elimelech, M. 2007 [Energy requirements of ammonia-carbon dioxide forward osmosis desalination](#). *Desalination* **207** (1–3), 370–382.
- Mi, B. & Elimelech, M. 2008 [Chemical and physical aspects of organic fouling of forward osmosis membranes](#). *J. Memb. Sci.* **320** (1–2), 292–302.
- Tang, C. Y., She, Q., Lay, W. C. L., Wang, R. & Fane, A. G. 2010 [Coupled effects of internal concentration polarization and fouling on flux behavior of forward osmosis membranes during humic acid filtration](#). *J. Memb. Sci.* **354** (1–2), 123–133.
- Xu, Y., Peng, X., Tang, C. Y., Fu, Q. S. & Nie, S. 2010 [Effect of draw solution concentration and operating conditions on forward osmosis and pressure retarded osmosis performance in a spiral wound module](#). *J. Memb. Sci.* **348** (1–2), 298–309.
- Zou, S., Gu, Y., Xiao, D. & Tang, C. Y. 2011 [The role of physical and chemical parameters on forward osmosis membrane fouling during algae separation](#). *J. Memb. Sci.* **366** (1–2), 356–362.

First received 20 May 2011; accepted in revised form 5 August 2011